

Design and Performance Analysis of An Energy-Efficient Uplink Carrier Aggregation Scheme

Fei Liu, Kan Zheng, Wei Xiang, and Hui Zhao

Abstract—Energy efficiency is of vital importance for telecommunications equipment in future networks, especially battery-constrained mobile devices. In the long term evolution-Advanced (LTE-Advanced) network, the carrier aggregation (CA) technique is employed to allow user equipment (UE) to use multiple carriers for high data rate communications. However, multi-carrier transmission entails increased power consumption at user devices in uplink networks. In this paper, we propose a new dynamic carrier aggregation (DCA) scheduling scheme to improve the energy efficiency of uplink communications. Two scheduling methods, i.e., serving the longest queue (SLQ) and round-robin with priority (RRP), are designed to reduce transmit power while maximizing the utilization of wireless resources. The proposed scheme is analyzed in terms of both the data rate and energy conservation. We build an ideally balanced system (IBS) to investigate the performance upper bound of the DCA scheme, and derive closed-form expressions. Simulation results demonstrate that the proposed scheme can not only enhance the energy efficiency but also perform closely to the optimal IBS.

Index Terms—Energy efficiency, carrier aggregation, carrier scheduling, LTE-Advanced.

I. INTRODUCTION

ENERGY efficiency in wireless networks is one of the major challenges for future information and communication technologies. To meet the demand of increasingly higher quality of service (QoS) requirements, more rapid data rates are expected, resulting in much higher energy cost at both user devices and base stations. However, slow advances in battery technologies mean that mobile devices can hardly deal with high energy consumption caused by increasingly popular mobile multimedia services [1]. For battery-constrained mobile terminals, uplink power consumption dominates the power budget for data transmission. As a consequence, reducing the uplink signal processing complexity and transmit power is indispensable in future wireless networks.

Aggregating frequency spectrum is one of the viable techniques to enhance data rates. Wide bandwidth, i.e., up to 100

Manuscript received September 26, 2012; revised November 1, 2012. This work was funded in part by China NSFC (No.61271183), National Basic Research Program of China (973 Program: 2012CB316005), Program for New Century Excellent Talents in University (NCET-11-0600), and the National Key Technology R&D Program of China under Grant 2013ZX03003005.

F. Liu, K. Zheng, and H. Zhao are with Key Lab of Universal Wireless Communications, Ministry of Education, Beijing University of Posts and Telecommunications, Beijing, 100088, China (e-mail: {liufei, zkan, hzhao}@bupt.edu.cn).

W. Xiang is with Faculty of the Engineering and Surveying, University of Southern Queensland, Toowoomba, QLD 4350, Australia (e-mail: wei.xiang@usq.edu.au).

Digital Object Identifier 10.1109/JSAC.2014.141202.

MHz, is required for the long term evolution-Advanced (LTE-Advanced) network to support high data rates [2]. As a result, carrier aggregation (CA) is employed by the 3rd Generation Partnership Project (3GPP) as a solution to bandwidth extension [3]. User equipment (UE) may simultaneously receive or transmit data on one or multiple component carriers (CCs). In the 3GPP Rel-8 specifications [4], each UE uses only one CC to communicate at one time. The energy cost and signalling overhead at the Rel-8 UEs are considerably reduced by not having to support bandwidths wider than 20 MHz. However, the UEs of Rel-10 can use multiple aggregated CCs to improve throughput inevitably with higher power consumption [5].

In the literature, several studies evaluate the issue of energy efficiency in uplink networks. The authors in [6] develop low-complexity energy-efficient link adaption and resource allocation schemes for uplink OFDMA systems. The average energy efficiency contours for single carrier uplink channel are analyzed in [7]. The problem of non-cooperative resource allocation in multi-cell uplink OFDMA systems is considered in [8] with respect to power conservation. Closed-form approximation of the energy efficiency versus spectral efficiency trade-off for the uplink systems is studied in [9] and [10]. To date, the studies of carrier scheduling and aggregation mainly focus on the performance of throughput and delay in the downlink network [11]–[13], but have seldom been conducted for the uplink network [14]. How to reduce the uplink power consumption at each user device, while enjoying the benefits of high data rates brought by the CA technique, is an important but under-explored research problem challenging the design of future LTE-Advanced networks.

In this paper, we introduce the joint carrier (JC) and independent carrier (IC) schemes and propose a new dynamic carrier aggregation scheme, with the aim of enhancing the throughput and energy efficiency (EE) performance in multi-carrier uplink networks. The major contributions of this paper are three-fold:

- A new energy efficiency metric is proposed for flow-based multi-carrier networks with elastic traffic. The normalized energy efficiency (NEE) is derived to improve the universality of the new EE metric, and is adopted to evaluate the EE performance of different schemes;
- We propose a novel dynamic carrier aggregation (DCA) scheme with two different scheduling methods, namely serving the longest queue (SLQ) and round-robin with priority (RRP), with the aim of increasing the data rate

and reducing the uplink power consumption;

- The carrier scheduling schemes are analyzed in terms of throughput and EE using queuing theory. Closed-form solutions for the upper and lower performance bounds are derived, serving as the benchmarks for various schemes. Backward compatibility and the requirements of the UE capabilities are analyzed and discussed.

An uplink LTE-Advanced network is simulated for evaluating the performance of the proposed scheme. Simulation results of the throughput and NEE of various schemes and the analytical solutions are presented and compared. The proposed DCA scheme can achieve significant improvement in the EE performance, which is close to the upper bound. We also calculate the signalling overhead of the proposed DCA schemes via the simulations.

The rest of this paper is organized as follows. The system model is described in Section II. A new carrier scheduling scheme is proposed in Section III. In Section IV, the performance metrics for energy efficiency are discussed for the flow-based multi-carrier uplink system. In Section V, we analyzed the theoretical performance of the proposed carrier scheduling scheme. The results of both theoretical analysis and simulations are presented in Section VI. Finally, Section VII draws the conclusion.

II. UPLINK TRANSMISSION SYSTEM MODEL

In an uplink OFDM-based network, there are multiple UEs communicating with the base station, termed the eNodeB (eNB) in the LTE-Advanced network, in a time-slotted fashion [5]. The eNB employs L CCs in the same frequency band with each CC having an identical bandwidth. The CA technique can support the aggregation of multiple CCs.

A dynamic flow model for elastic traffic is assumed, where each UE transmits its flows with finite lengths to the eNB [15]. Each arrival flow is transmitted via uplink channels independently. The arrival flows to the network follow a Poisson process with an average arrival rate of λ . The flow size is exponentially distributed as shown below.

$$P\{F^{(n)} \leq a\} = 1 - e^{-a/\bar{F}}, a \in \mathbb{N}^+, \quad (1)$$

where $F^{(n)}$ is the file length of user n , $\bar{F} = \mathbb{E}[F^{(n)}]$ is the average flow size, and \mathbb{N}^+ is the set of integers larger than 0.

Each CC is comprised of K resource blocks (RBs). The RBs of a CC are distributed to multiple UEs by its resource scheduler (RS) to transmit the uplink flows of the UEs. Each UE is Rel-10 compliant which can use multiple CCs simultaneously with the CA technique. However, transmission through multiple CCs can increase the computational complexity and power consumption at UE. In terms of computational complexity, a UE has to process the encoding and modulation for uplink transmission with more than one single CC. Meanwhile, the usage of multiple CCs is obviously not energy efficient.

At each time slot, the RS allocates RBs to the given UEs according to a scheduling strategy. In this paper, the RBs are equally divided and allocated to the related UEs circularly through the round-robin (RR) strategy, such that the UEs share the radio resources of one or multiple aggregated CCs fairly.

We model the uplink channel of each CC with consideration of uplink power control. We denote $P_l^{(n)}$ as the uplink transmit power of UE n using a single CC l to communicate with the eNB. Thus, the power on each RB is $P_l^{(n)}/K$ ignoring power allocation for relatively flat fading within each CC. Then the instantaneous signal-to-interference-plus-noise ratio (SINR) on RB k at CC l of UE n can be expressed as

$$\gamma_{l,k}^{(n)} = \frac{\alpha_l^{(n)} |h_{l,k}^{(n)}|^2 P_l^{(n)}/K}{I_{l,k} + \delta^2}, 1 \leq l \leq L, 1 \leq k \leq K, \quad (2)$$

where $\alpha_l^{(n)}$ represents the path loss attenuation factor of UE n using CC l , $h_{l,k}^{(n)}$ denotes the independent complex fading channel gain on RB k at CC l of UE n , modeled as $h_{l,k}^{(n)} \sim \mathcal{CN}(0, \sigma^2)$ ¹ with $\sigma^2 = \mathbb{E}[|h_{l,k}^{(n)}|^2]$, δ^2 is the noise power of the additive white Gaussian noise (AWGN), and $I_{l,k}$ is the average power of the received inter-cell interference on RB k at CC l , modeled as

$$\begin{aligned} I_{l,k} &= \mathbb{E} \left[\sum_{i \in N_B} \sum_{n_i} \beta_l^{(n_i)} |h_{l,k}^{(n_i)}|^2 P_l^{(n_i)}/K \right] \\ &= \sum_{i \in N_B} \sum_{n_i} \int_0^\infty \frac{\sigma^2}{K} P_l^{(n_i)} \beta_l^{(n_i)} g_i(\beta_l^{(n_i)}) d\beta_l^{(n_i)}, \quad (3) \end{aligned}$$

where $i \in N_B$ is the index of an eNB in the set of the neighboring eNBs N_B , in which the uplink signal of its UE n_i causes interference with transmit power $P_l^{(n_i)}$, $\beta_l^{(n_i)}$ represents the path loss attenuation factor from UE n_i to the interfered eNB, and $g_i(\beta_l^{(n_i)})$ is the probability distribution function (PDF) of $\beta_l^{(n_i)}$, which is related to the user distribution. We rewrite $I_{l,k}$ as I_l since the fast fading coefficient of each subchannel is estimated at the same level with the parameter $\sigma^2 = \mathbb{E}[|h_{l,k}^{(n)}|^2]$.

The close-loop power control is adopted for uplink transmission [16]. The target average SINR is expressed as

$$\bar{\gamma}_0 = \mathbb{E} \left[\gamma_{l,k}^{(n)} \right] = \frac{\alpha_l^{(n)} \sigma^2 \mathbb{E} \left[P_l^{(n)} \right]}{(I_l + \delta^2) K}, 1 \leq l \leq L. \quad (4)$$

Thus, the controlled average uplink transmit power of user n using CC l can be calculated as

$$\bar{P}_l^{(n)} = \mathbb{E} \left[P_l^{(n)} \right] = \frac{(I_l + \delta^2) K \bar{\gamma}_0}{\alpha_l^{(n)} \sigma^2}, 1 \leq l \leq L. \quad (5)$$

It is noted that the instantaneous SINR of each UE can not be guaranteed with the target $\bar{\gamma}_0$ by nonideal power control due to rapid change of radio channels. This nonideality of the close-loop power control is calculated and presented in Section VI. Thus, the power control by obtained $\bar{P}_l^{(n)}$ can only maintain an average SINR level $\bar{\gamma}_0$ of UE n on CC l [16].

The achievable data rate on RB k at CC l of UE n is

$$C_{l,k}^{(n)} = N_{sc} S_{eff} \log_2 \left(1 + \gamma_{l,k}^{(n)} \right) / T_s, \quad (6)$$

where N_{sc} is the number of subcarriers in each RB, S_{eff} is the number of effective OFDM symbols of one LTE-Advanced frame in the time domain, and T_s is the frame length [5].

¹A circularly symmetric complex Gaussian random value x with mean π and covariance τ is denoted by $x \sim \mathcal{CN}(\pi, \tau)$.

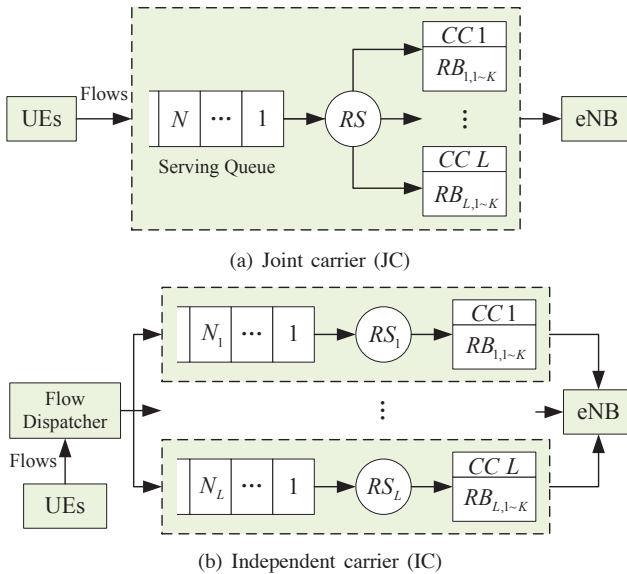


Fig. 1. System models of the JC and IC schemes.

III. CARRIER SCHEDULING SCHEMES

As mentioned in Section I, it is a significant issue to decrease the transmit power while fully utilizing the multiple CCs with the CA technique. In this section, we first introduce the framework of CA-based uplink scheduling systems through describing two carrier scheduling schemes, namely joint carrier (JC) and independent carrier (IC) [11], followed by the proposal of a dynamic carrier aggregation (DCA) scheme which is capable of improving the EE performance.

A. Joint Carrier (JC)

In JC, each UE is served by all the CCs, i.e., the data of any current flow can be transmitted over all the L CCs. As illustrated in Fig. 1(a), there is a single resource scheduler (RS) assigning the RBs of all the L CCs to the flows. Such a centralized processing mechanism leads to full resource utilization [13], [17]. Therefore, maximum throughput is attainable through JC. However, each UE has to maintain connection with all the CCs simultaneously. Thus, the effectiveness of JC is largely limited while considering the power budget.

B. Independent Carrier (IC)

In IC, each UE can only use a single CC. When a new flow arrives at the system, a flow dispatcher immediately assigns it to a CC, as shown in Fig. 1(b). Then, the data of this flow can only be transmitted over the assigned CC. There are independent RS and a flow queue for each CC.

In IC, each UE incurs minimum power consumption since only a single CC is used for the transmission of its flow. However, the traffic on all the CCs is not always balanced, which may lower the overall transmission capacity of the whole system. Some CCs may become idle if their queues are empty, while the other CCs are busy at serving their own flows. In order to balance the traffic load across the CCs, the dispatcher needs to sensibly select an allocation strategy, e.g., random allocation (RA), round-robin (RR), or

joint the shortest queue (JSQ) [17]. With the RA approach, the dispatcher assigns arrival flows to different CCs with given probabilities. RR is a fair allocation algorithm, where flows are assigned to all the CCs circularly. As for the JSQ method, it takes into account the queue length of each CC, and allocates an arrival flow to the queue with the least number of flows.

C. Dynamic Carrier Aggregation (DCA)

When the IC scheme is applied, a CC stays idle so long as all its assigned flows have been served, although there may be flows assigned to other CCs still being served. On the other hand, the JC approach offers a higher data rate than its IC counterpart at the expense of more transmit energy cost. We propose a DCA scheme which can achieve the same maximum throughput as JC with much less power consumption.

With a certain dispatching strategy, arrival flows are allocated by a dispatcher to the queue at each CC. The corresponding UE of a flow in the queue of a CC chooses this CC as its primary component carrier (PCC), with which the UE transmits signaling information alongside flow data. A UE has only a single PCC at a time, which remains unchanged during transmission since activation and deactivation of the PCC are very time-consuming in the LTE-Advanced systems [5].

With the proposed DCA scheme, each CC first serves the flows in its own queue when it is not empty. Whenever a queue of any CC becomes empty, the concerned CC, dubbed the supplementary component carrier (SCC), is able to help other CCs using the aggregation technique. In this way, the total capacity of all the CCs can be fully utilized to serve the nonempty queues. Furthermore, we propose two CC cooperation approaches with the DCA scheme in the following.

1) *Serving the Longest Queue (SLQ)*: All the SCCs are aggregated with the PCC with the longest queue. If more than one PCC has the same longest queue length, the SCCs are allocated to any one of them randomly. For illustration purposes, an example of the system with four CCs using the SLQ method is shown in Fig. 2. The queues of CCs 2 and 3 are empty, i.e., the queue length $N_2 = N_3 = 0$, while those of CCs 1 and 4 are nonempty. Then, CCs 2 and 3 are used as the SCCs. CC 1 is aggregated with CCs 2 and 3 in the event that the queue of CC 1 is longer than that of CC 4, i.e., $N_1 > N_4$. Then, the RBs of CCs 2 and 3 are merged with that of CC 1, altogether serving the flows in the queue of CC 1.

2) *Round-robin with Priority (RRP)*: The PCCs are first sorted according to their queue lengths before being aggregated with the SCCs. The SCCs are circularly allocated to the ordered PCCs with the RR principle. In this way, the PCC with a longer queue length has a higher priority to be aggregated with one or more SCCs. However, the PCC with a shorter queue length also has the opportunity to be aggregated with SCCs when there are more than one SCC. Unlike the SLQ scheme in Fig. 2, CC 2 is firstly allocated to CC 1 because CC 1 has a longer queue length. Next, CC 3 helps CC 4.

In CA-based LTE-Advanced systems, the SCC switch procedure incurs a signalling overhead by occupying several frames for SCC setup [16]. Each time a UE accesses to an aggregated SCC, it spends a certain amount of transmission

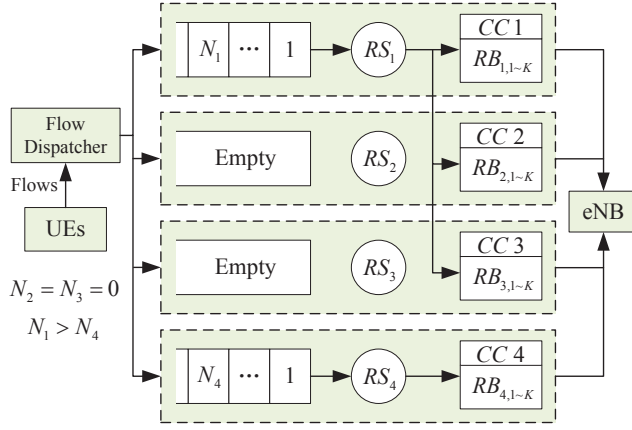


Fig. 2. One example of the serving the longest queue (SLQ) scheme.

bits for the SCC switch and loses corresponding data rate. The impact of this switch procedure on the performance of throughput and EE is considered and evaluated in Section VI.

IV. ENERGY EFFICIENCY METRIC

In this section, we present the definition and derivation of the normalized form of the EE metric for multi-carrier systems with elastic traffic. Moreover, the method of evaluating the EE performance of realistic systems is also presented.

A. Analytical EE performance

We first introduce a widely used energy efficiency indicator for transmission systems [18], bits-per-joule (b/J), defined as

$$U(R) = \frac{R}{P(R)}, \quad (7)$$

where R is the data rate, and $P(R)$ is the transmit power required to achieve rate R .

Based on the models described in Section II and the scheduling schemes in Section III, we further derive the bits-per-joule in (7) to obtain the analytical EE performance. With the RR strategy for RB distribution for UEs within each CC, the queuing model of the CC can be modeled as a processor-sharing (PS) queue. We first calculate the serving rates of the CCs. Let $\bar{C}_{l,k}^{(n)} = \mathbb{E}[C_{l,k}^{(n)}]$ be the average transmission rate on RB k at CC l of UE n , i.e.,

$$\bar{C}_{l,k}^{(n)} = \frac{S_{eff} N_{sc}}{T_s} \int_0^\infty \log_2(1 + \gamma_{l,k}^{(n)}) f(\gamma_{l,k}^{(n)}) d\gamma_{l,k}^{(n)}, \quad (8)$$

where $f(\gamma_{l,k}^{(n)})$ is the PDF of $\gamma_{l,k}^{(n)}$. With the Rayleigh fading channel, the instantaneous SINR $\gamma_{l,k}^{(n)}$ follows an exponential distribution. Its PDF is given by

$$f(\gamma_{l,k}^{(n)}) = \frac{1}{\bar{\gamma}_0} \exp\left(-\frac{\gamma_{l,k}^{(n)}}{\bar{\gamma}_0}\right), \quad (9)$$

where $\bar{\gamma}_0 = \mathbb{E}[\gamma_{l,k}^{(n)}]$ is the target average SINR. Thus, the average data rate for UE n on CC l is given by

$$\bar{C}_l^{(n)} = \sum_{k=1}^K \bar{C}_{l,k}^{(n)}. \quad (10)$$

As derived by (8)-(10), $\bar{C}_l^{(n)}$ is only related to the target SINR $\bar{\gamma}_0$, rewritten as \bar{C} . Therefore, the average flow serving rate per CC is identical and can be calculated as

$$\mu_{cc} = \bar{C}/\bar{F}. \quad (11)$$

Thus, the total capacity of all the CCs is

$$\mu = L\mu_{cc}. \quad (12)$$

Then, we calculate the mean power consumption at users using CC l from the system point of view as follows

$$\begin{aligned} \bar{P}_l &= \int_0^\infty \bar{P}_l^{(n)} g(\alpha_l^{(n)}) d\alpha_l^{(n)} \\ &= \frac{(I_l + \delta^2) K \bar{\gamma}_0}{\sigma^2} \int_0^\infty \frac{g(\alpha_l^{(n)}) d\alpha_l^{(n)}}{\alpha_l^{(n)}}, \end{aligned} \quad (13)$$

where $g(\alpha_l^{(n)})$ is the PDF of the path loss attenuation factor of UE n , which is related to the distribution of the UE locations. Since all UEs can equiprobably using any CCs, their mean transmit power on every CC can be calculated for estimation of the average level of power consumption, i.e.,

$$P_{cc} = \frac{1}{L} \sum_{l=1}^L \bar{P}_l. \quad (14)$$

Thus, the average bits-per-joule of the UE flows can be written as

$$U = \frac{\bar{R}}{\bar{L}P_{cc}} = \frac{\bar{F}}{\bar{D}} \cdot \frac{\mu_{cc}}{\bar{L}P_{cc}\mu_{cc}} = \frac{\bar{F}\mu_{cc}}{P_{cc}} \left(\frac{1}{\bar{L}\mu_{cc}\bar{D}} \right), \quad (15)$$

where \bar{R} is the data rate of the flows, \bar{L} is the average number of CCs used during the flows' transmission, \bar{D} is the average transmission time of each flow.

U in (15) can be adopted to evaluate the analytical EE performance of various carrier scheduling schemes. However, in various application scenarios, the transmit power is related to the radio channel quality and system configurations, while the flow length is determined by the type of mobile service. In order to improve the universality of U to compare each scheduling schemes fairly, we derive its normalized form as follows. We denote the energy efficiency coefficient (EEC) by

$$A_c = \frac{\bar{F}\mu_{cc}}{P_{cc}}, \quad (16)$$

and define the normalized energy efficiency (NEE) as

$$\varphi = \frac{1}{\bar{L}\mu_{cc}\bar{D}}. \quad (17)$$

If the flow of each UE monopolizes the \bar{L} CCs that it uses without sharing with any other UEs, it can obtain the whole capacity and throughput of the \bar{L} CCs, i.e.,

$$\bar{R} = \bar{F}(\bar{L}\mu_{cc}).$$

However, the fact is that there always be multiple UEs sharing the \bar{L} CCs, such that no UE can occupy the overall capacity of the \bar{L} CCs. As such, we have

$$\bar{R} = \frac{\bar{F}}{\bar{D}} \leq \bar{F}(\bar{L}\mu_{cc}) \Rightarrow \bar{D} \geq \frac{1}{\bar{L}\mu_{cc}}.$$

Therefore, the following relationships for NEE φ and U hold

$$\begin{aligned} 0 < \varphi \leq 1, \\ U = A_c \varphi \leq A_c. \end{aligned}$$

Thus, the EEC A_c indicates the maximum bits-per-joule value, while the NEE φ implies the achievable proportion of A_c .

B. NEE Evaluation in Practical Systems

In realistic multi-carrier systems, the actual serving rate $\hat{\mu}_{cc}$ is measurable by computing the average flow leaving interval. Meanwhile, the average number of connected CCs \hat{L} of each flow and the flow delay \hat{D} can be statistically calculated. Thus, the NEE measured in a practical system is

$$\hat{\varphi} = \frac{1}{\hat{L}\hat{\mu}_{cc}\hat{D}}. \quad (18)$$

In Section V, we analyze the theoretical EE performance of different carrier scheduling schemes according to (17). Then, in Section VI, the measured NEE in (18) is obtained via simulation and compared with the analytical result.

V. ANALYSIS OF THEORETICAL TRANSMISSION AND ENERGY EFFICIENCY PERFORMANCE

A. Joint Carrier (JC)

Considering the arriving and departing processes with the JC scheme, the PS queueing system is $M/G/1-PS$. The solution of the average transmission time is given in [19], and proved independent of the departing process. Moreover, the steady-state probability distribution of the queue length of an $M/G/1-PS$ system and the average flow delay are consistent with those of $M/M/1-PS$ [19]. Thus, the system can be formulated as an $M/M/1$ queueing model with an arrival rate of λ for the JC scheme. The average serving rate is the sum of the capacity of all the CCs, i.e., $\mu = L\mu_{cc}$. Define the traffic load of the network as $\rho = \lambda/\mu$. The queueing system keeps working with a limited overall queue length, i.e., $N < \infty$, under the condition of $0 \leq \rho < 1$.

Therefore, the average transmission time and average data rate can be calculated by

$$\begin{aligned} \bar{D}_{JC} &= \frac{1}{\mu - \lambda}, \\ \bar{R}_{JC} &= \frac{\bar{F}}{\bar{D}_{JC}} = \bar{F}L\mu_{cc}(1 - \rho). \end{aligned} \quad (19)$$

In the JC scheme, the average number of the CCs used by each flow is the maximum, i.e., $\bar{L}_{JC} = L$. Thus, the power consumption is the highest. The bits-per-joule and NEE of the JC scheme are given by

$$\begin{aligned} U_{JC} &= \frac{\bar{R}_{JC}}{P_{cc}\bar{L}_{JC}} = \frac{\bar{F}\mu_{cc}}{P_{cc}}(1 - \rho), \quad (20) \\ \varphi_{JC} &= 1 - \rho. \quad (21) \end{aligned}$$

The NEE of JC is only related to the traffic load ρ in a linear relationship, and varies in the range of $0 < \varphi_{JC} \leq 1$. The JC scheme can only be used for the Rel-10 UE [3], which is capable of transmitting data through multiple CCs, and thus provides no backward compatibility for the Rel-8 UE.

B. Independent Carrier (IC)

The system can be formulated as L parallel PS servers corresponding to the L CCs. The serving rate of each PS server is $\mu_l = \mu_{cc}$. There is a dispatcher routing flows to the servers so that the arrival flow rate at server l is λ_l . Various dispatch algorithms impact on the system performance differently.

1) *Random Allocation (RA)*: With the RA algorithm, flows probabilistically independently arrive at CC l with probability $\beta_l \geq 0$, where $\sum_{l=1}^L \beta_l = 1$. Then, the arrival process at each server is still Poisson and its rate is $\lambda_l = \beta_l\lambda$. Thus, each serving queue is $M/G/1-PS$, consistent with the whole system with the JC scheme [20]. Specially, when we assume the same dispatching probability of each CC, i.e., $\beta_l = 1/L$, the transmission performance can be derived as follows

$$\begin{aligned} \bar{D}_{IC-RA} &= \frac{L}{\mu - \lambda}, \\ \bar{R}_{IC-RA} &= \frac{\bar{F}}{\bar{D}_{IC-RA}} = \bar{F}\mu_{cc}(1 - \rho). \end{aligned} \quad (22)$$

The average transmission time of flows with IC-RA is L times of that with JC. However, since the UE with the IC scheme only uses a single CC to communicate with the eNB, its power consumption is $1/L$ of that with JC. Thus, the EE performance of IC-RA is the same as that of JC, i.e.,

$$U_{IC-RA} = \frac{\bar{R}_{IC-RA}}{P_{cc}\bar{L}_{IC}} = \frac{\bar{F}\mu_{cc}}{P_{cc}}(1 - \rho), \quad (23)$$

$$\varphi_{IC-RA} = 1 - \rho. \quad (24)$$

2) *Round-robin (RR)*: The interval of the arrival flows of each queue is Erlang distributed [20] with the RR algorithm. Thus, each CC behaves like an $E_L/G/1-PS$ system. Its analytical performance is attainable only when the serving process satisfies certain conditions. We use the solution of the $E_L/M/1-PS$ system with the same arrival process and average serving rate μ_{cc} as an approximation. As indicated in [20], its performance is better than that of the $E_L/G/1-PS$ system, when the serving time of the process G has a larger variance than that of the Poisson process M , and thus can be regarded as an upper bound.

The solution of the $E_L/M/1-PS$ queueing system can be obtained according to [21]. As such, the average transmission time and average data rate are derived as follows

$$\begin{aligned} \bar{D}_{IC-RR} &= \frac{L}{\mu} \frac{1}{1 - \eta}, \\ \bar{R}_{IC-RR} &= \frac{\bar{F}}{\bar{D}_{IC-RR}} = \bar{F}\mu_{cc}(1 - \eta), \end{aligned} \quad (25)$$

where η denotes the unique root in the unit circle of (28) below. The PDF of the interval between the arrival flows at each CC is given by

$$p(t) = \frac{\lambda(\lambda t)^{L-1}}{(L-1)!} e^{-\lambda t}, t \geq 0. \quad (26)$$

Applying the Laplace transform to (26) gives rise to

$$f_s(s) = \int_0^{+\infty} p(t) e^{-st} dt = \left(\frac{\lambda}{\lambda + s} \right)^L. \quad (27)$$

According to the method in [21] of solving the average sojourn time in the $G/M/1-PS$ system, equation (5) in [21] can be written as

$$\eta = f_s(\mu_{cc} - \mu_{cc}\eta) = \left(\frac{\lambda}{\lambda + \mu_{cc} - \mu_{cc}\eta} \right)^L \quad (28)$$

$$\implies \lambda^L = \eta(\lambda + \mu_{cc} - \mu_{cc}\eta)^L.$$

The minimal non-negative solution of (28) is η for (25). Then, the bits-per-joule value and NEE of the IC-RR system can be calculated as

$$U_{IC-RR} = \frac{\bar{R}_{IC-RR}}{P_{cc}\bar{L}_{IC}} = \frac{\bar{F}\mu_{cc}}{P_{cc}}(1 - \eta), \quad (29)$$

$$\varphi_{IC-RR} = 1 - \eta. \quad (30)$$

Similar to that of the IC-RA system, the NEE of IC-RR also decreases with increase of the traffic load ρ .

3) *Joint the Shortest Queue (JSQ)*: The JSQ method allocates a new arriving flow to the serving queue with the least number of flows backlogged. So, the arrival process of each queue is not independent [22]. By using a special single-queue approximation (SQA) method, the performance of the JSQ queueing system can be analyzed according to [22]. Due to the near insensitivity of $M/G/L/JSQ-PS$ to the processing time distribution, we use $M/M/L/JSQ-PS \approx M/G/L/JSQ-PS$, as an approximation. And with the SQA method in [22], we have $M/M/L/JSQ-PS \stackrel{SQA}{\cong} M_N/M/1$.

The average queue length for various ρ and the numbers of CCs L , denoted by $\bar{N}_{IC-JSQ} = \varsigma(L, \rho)$, are given in the Table 2 in [23]. With the average queue length, the transmission performance can be derived according to the Little Theorem as follows

$$\bar{D}_{IC-JSQ} = \frac{\varsigma(L, \rho)}{\lambda},$$

$$\bar{R}_{IC-JSQ} = \frac{\bar{F}}{\bar{D}_{IC-JSQ}} = \frac{\lambda\bar{F}}{\varsigma(L, \rho)}. \quad (31)$$

Then, the EE performance of IC-JSQ can be computed as

$$U_{IC-JSQ} = \frac{\bar{R}_{IC-JSQ}}{P_{cc}\bar{L}_{IC}} = \frac{\bar{F}\mu_{cc}}{P_{cc}} \left[\frac{\rho L}{\varsigma(L, \rho)} \right], \quad (32)$$

$$\varphi_{IC-JSQ} = \frac{\rho L}{\varsigma(L, \rho)}. \quad (33)$$

The JSQ dispatching algorithm can balance the flow traffic on the CCs better than its RA and RR counterparts. This point is discussed and validated in Section VI.

C. Dynamic Carrier Aggregation (DCA)

The system employing the proposed DCA scheme can be modeled as a special $M/G/\bar{L}-PS$ system. Different from the IC scheme, the number of serving lines \bar{L} and the capacity of them vary depending on the carrier aggregation state. According to the conservation law for time-shared systems in [20], the DCA system ensures the full utilization of carrier resources, because no transmission bandwidth of the carriers is wasted when there are still flows in the queues. Thus, the average queueing performance of the DCA scheme is the same as that of the JC scheme and its transmission performance can

be derived as in (19). Moreover, the departing process is also a Poisson one due to the insensitivity of the PS queueing system, as well as the fact that DCA can be regarded as a combination of Poisson processes [24]. Thus, the steady-state probability of each state of the overall queue length can be solved readily as follows

$$P\{N\} = (1 - \rho)\rho^N, \quad N = 0, 1, 2, \dots, \quad (34)$$

where $P\{N=0\}$ is the idle state probability of the system with no flow in the queue, and $P\{N\}$ is the state probability of N flows backlogged in the system [20].

To achieve the same delay and throughput performance, the less number of SCCs each UE uses, the more transmission energy is saved for mobile devices. A UE served by only the PCC has the lowest power consumption in comparison with a UE served by both its PCC and SCCs. Therefore, the number of active SCCs plays a critical role in evaluating the EE performance of various carrier scheduling schemes.

We build an ideally balanced system (IBS) to analyze the DCA scheme, in which a UE can switch its PCC freely to reduce the probability of using the aggregated SCCs. To balance the flow traffic on each queue to the maximum extent, if there are multiple users' flows served in a CC queue and some other CCs' queues are empty, some of the UEs can change their PCCs to the idle CCs ignoring the limit in the real operation process. Therefore, users can never use multiple carriers unless there are only a few flows, which are less than the number of CCs. When there are L or more flows being transmitted, each UE can use only the PCC to communicate with the aim of reducing energy consumption. However, when the number of active users is less than that of the CCs, to guarantee the full utilization of wireless resource, some UEs can use the SCCs aggregated with their PCCs in accordance with a certain DCA scheme. Different aggregation methods, i.e., SLQ and RRP, may result in various SCC aggregation states.

For ease of analysis, no signalling overhead and delay for aggregation operation in the IBS are considered. This IBS is impractical but has the best balance performance, and can consequently reduce the chance to use the SCCs. So the EE performance of the IBS is treated as an upper bound of the DCA scheme with various dispatching algorithms. To evaluate the backward compatibility and requirements of UE capability, the probability of using only the PCC and the maximum number of CCs possibly used by each UE are also calculated.

1) *Average Number of CCs Used by Each Flow (\bar{L}) in the DCA-IBS*: We compute the average number of the CCs used during the transmission process of each flow in the DCA-IBS to estimate the energy consumption at the UEs. For any DCA scheme in the IBS with full utilization, all the CCs with empty queues are used as the SCCs under SLQ or RRP. Therefore, the number of the SCCs in each state of the queue length is determined only by N . Denoting by $L_{DCA-IBS}^*$ the number of the SCCs in each queue length state, we have

$$L_{DCA-IBS}^* = \begin{cases} L - N, & 0 < N < L, \\ 0, & L \leq N. \end{cases} \quad (35)$$

Then the expectation of $L_{DCA-IBS}^*$ under the busy condition of the system, i.e., $N > 0$, is computed as

$$\mathbb{E}[L_{DCA-IBS}^*|N > 0] = \sum_{N=1}^{L-1} (L-N)P\{N|N > 0\} = \frac{L-1-L\rho+\rho^L}{1-\rho}. \quad (36)$$

When the system is busy, the average number of the backlogged flows is given by

$$\mathbb{E}[N|N > 0] = \frac{1}{1-\rho}. \quad (37)$$

Then, the average number of the SCCs used by each flow in the DCA-IBS can be calculated as

$$\bar{L}_{DCA-IBS}^* = \frac{\mathbb{E}[L_{DCA-IBS}^*|N > 0]}{\mathbb{E}[N|N > 0]} = L-1-L\rho+\rho^L. \quad (38)$$

Besides the SCCs, every UE has one single PCC. Therefore, \bar{L} for the DCA-IBS is

$$\bar{L}_{DCA-IBS} = \bar{L}_{DCA-IBS}^* + 1 = L(1-\rho) + \rho^L. \quad (39)$$

2) *NEE of the DCA-IBS*: The DCA scheme has the same transmission performance as JC in (19). Thus, the EE performance of the DCA-IBS is given as follows according to (15),

$$U_{DCA-IBS} = \frac{\bar{R}_{DCA}}{P_{cc}\bar{L}_{DCA-IBS}} = \frac{\bar{F}\mu_{cc}}{P_{cc}} \left[1 + \frac{\rho^L}{L(1-\rho)} \right]^{-1}, \quad (40)$$

$$\varphi_{DCA-IBS} = \left[1 + \frac{\rho^L}{L(1-\rho)} \right]^{-1}. \quad (41)$$

The NEE is an increasing function of L and a decreasing one of ρ . Specially, if there is only a single CC in the system, i.e., $L = 1$, then $\varphi_{DCA-IBS} = 1 - \rho$. This is consistent with the NEE of JC, since all the CCs are aggregated and can be regarded as one with the JC scheme.

3) *Probability of Using Only the PCC in the IBS*: The LTE Rel-8 UE can use only one single CC at a time. Therefore, the probability of using only the PCC is a useful parameter to assess the backward compatibility for the Rel-8 UEs in the IBS. Let N° be the number of UEs using only the PCC in each state of the queue length. The probability of using only the PCC without any SCCs is denoted by $P\{L^* = 0\}$.

Firstly, we calculate the probability for the SLQ-IBS. $N_{SLQ-IBS}^\circ$ in each queue length state N is given by

$$N_{SLQ-IBS}^\circ = \begin{cases} N-1, & 1 \leq N < L, \\ N, & L \leq N. \end{cases} \quad (42)$$

Then the expectation of $N_{SLQ-IBS}^\circ$ when the system is busy is derived according to (34),

$$\mathbb{E}[N_{SLQ-IBS}^\circ|N > 0] = \frac{\rho + \rho^{L-1} - \rho^L}{1-\rho}.$$

So, the probability of UEs using only the PCC is

$$P\{L_{SLQ-IBS}^* = 0\} = \frac{\mathbb{E}[N_{SLQ-IBS}^\circ|N > 0]}{\mathbb{E}[N|N > 0]} = \rho + \rho^{L-1} - \rho^L. \quad (43)$$

The analysis of $P\{L_{RRP-IBS}^* = 0\}$ in the RRP-IBS depends on whether L is even or odd. When L is even,

$$N_{RRP-IBS}^\circ = \begin{cases} 0, & 1 \leq N \leq \frac{L}{2}, \\ 2N-L, & \frac{L}{2} < N < L, \\ N, & L \leq N. \end{cases} \quad (44)$$

When there are flows in the system, the mean value of (44) is

$$\mathbb{E}[N_{RRP-IBS}^\circ|N > 0] = \frac{2\rho^{L/2} - \rho^L}{1-\rho}.$$

Thus, the probability of the UEs using only the PCC in the RRP-IBS, when L is an even number, can be derived as

$$P\{L_{RRP-IBS}^* = 0\} = \frac{\mathbb{E}[N_{RRP-IBS}^\circ|N > 0]}{\mathbb{E}[N|N > 0]} = 2\rho^{L/2} - \rho^L. \quad (45)$$

Similarly, if L is odd, we arrive at the following

$$N_{RRP-IBS}^\circ = \begin{cases} 0, & 1 \leq N \leq \frac{L-1}{2}, \\ 2N-L, & \frac{L-1}{2} < N < L, \\ N, & L \leq N. \end{cases} \quad (46)$$

When there are flows in the system, the mean value of (46) is

$$\mathbb{E}[N_{RRP-IBS}^\circ|N > 0] = \frac{\rho^{(L-1)/2} + \rho^{(L+1)/2} - \rho^L}{1-\rho}.$$

Thus, the probability of the UEs using only the PCC in the RRP-IBS, when L is odd, can be derived as

$$P\{L_{RRP-IBS}^* = 0\} = \frac{\mathbb{E}[N_{RRP-IBS}^\circ|N > 0]}{\mathbb{E}[N|N > 0]} = \rho^{(L-1)/2} + \rho^{(L+1)/2} - \rho^L. \quad (47)$$

Specially, when L is 1, 2 or 3, i.e., there are 1, 2 or 3 CCs in the uplink system, the SLQ and RRP schemes result in the same scheduling method. When $L = 1$, we have

$$P\{L_{SLQ-IBS}^* = 0\}_{L=1} = P\{L_{RRP-IBS}^* = 0\}_{L=1} = 1.$$

All the UEs always use a single PCC, since there is only one CC available in the system. When $L = 2$ and 3, we have

$$P\{L_{SLQ-IBS}^* = 0\}_{L=2} = P\{L_{RRP-IBS}^* = 0\}_{L=2} = 2\rho - \rho^2,$$

$$P\{L_{SLQ-IBS}^* = 0\}_{L=3} = P\{L_{RRP-IBS}^* = 0\}_{L=3} = \rho + \rho^2 - \rho^3.$$

The above results confirm the consistency of SLQ and RRP when $L = 1, 2$ and 3.

When there exist more than 3 CCs, it is easy to derive the relationship as follows,

$$P\{L_{SLQ-IBS}^* = 0\}_{L>3} \geq P\{L_{RRP-IBS}^* = 0\}_{L>3}.$$

This means that SLQ always has a higher $P\{L^* = 0\}$ than RRP when $L > 3$. Therefore, SLQ has better backward compatibility than RRP for the LTE Rel-8 UEs.

TABLE I
SIMULATION PARAMETERS

Parameter	Value
Inter-cell distance (ISD)	500 m
Number of CCs (L)	2, 4
Carrier frequency (f_l)	2 GHz
Number of RBs per CC (K)	25
Bandwidth per CC	5 MHz
Effective symbols per frame (S_{eff})	10
Number of sub-carriers per RB (N_{sc})	12
Frame length (T_s)	1 ms
SCC switch procedure	10 frames
Target average SINR ($\bar{\gamma}_0$)	0 dB
Channel model	UMa
Thermal noise spectral density	-174 dBm/Hz
Fast fading coefficient (σ^2)	1.0
Average flow size (F)	1.0 Mb

4) *Maximum Number of the CCs Used by Each UE*: Due to the limitation of transmit power and processing capacity of UEs for multi-carrier communications, the maximum number of the CCs required by the DCA scheme is expected to be less. Decreasing the maximum power consumption at a UE can ensure that it works within its capability. Therefore, we give the discussion about the maximum number of the CCs used by each UE with SLQ and RRP as follows.

We ignore the condition of $N = 1$ because both SLQ and RRP allocate $L - 1$ SCCs aggregated with the only one PCC that the UE uses in the IBS when $N = 1$. When there are more than one flow, i.e., $N > 1$, the range of the SCC number aggregated for each UE, i.e., L^* , varies with different DCA principles. For the SLQ method, $L_{SLQ}^* \in \{0, 1, \dots, L - 2\}$. As for RRP, $L_{RRP}^* \in \{0, 1, \dots, \lceil L/2 \rceil - 1\}$. Thus, when $N > 1$, the maximum number of the CCs used by each UE for SLQ is $L - 1$, while for RRP it is $\lceil L/2 \rceil$, which may be less.

From the above discussions, the features of SLQ and RRP can be summarized as follows: With SLQ, UEs have higher probabilities to only use the PCC to communicate. But it may lead to higher maximum power consumption. With RRP, UEs can hardly use only the PCC but have to aggregate the SCCs. However, the requirement of the maximum capability of the device is lower, especially when more CCs are available.

VI. SIMULATION AND NUMERICAL RESULTS

In this section, the performance of various carrier scheduling schemes in the LTE-Advanced system is obtained through simulations with the parameters listed in Table I. The urban macro (UMa) wireless environment is used as the channel model [5]. The path loss attenuation factor is modeled as

$$\alpha_l^{(n)} = - \left[128.1 - f_l + 37.6 \log_{10} \left(d^{(n)} \right) \right] \quad (\text{in dB}),$$

where $d^{(n)}$ is the distance between user n and the eNB in km, and f_l is the carrier frequency.

We first calculate the analytical transmission capacity per CC according to (11), which is $\mu_{cc} = 2.5811 \text{ s}^{-1}$. Then, we set the arrival rate λ according to the total capacity of the uplink network, i.e., $\mu = L\mu_{cc}$, to maintain the traffic load of $0 < \rho < 1$. The average transmit power per CC of each UE with uplink power control is analyzed to be $P_{cc} = 15.06 \text{ dBm}$. The simulation results of the cumulative distribution function

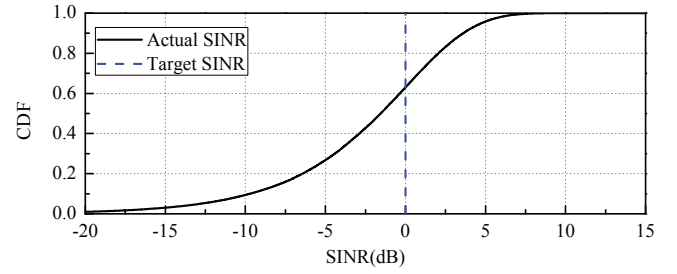


Fig. 3. CDF of the SINR with nonideal uplink power control.

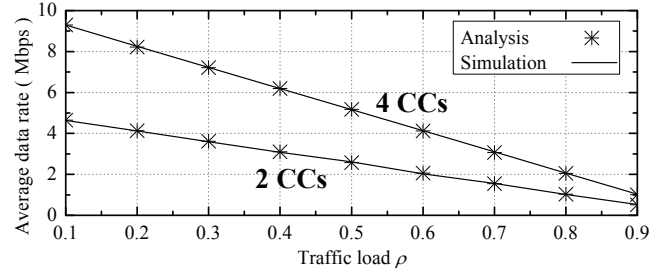


Fig. 4. Analytical and simulation results of the average data rates in the systems with 2 and 4 CCs using the JC scheme.

(CDF) of the SINR is presented in Fig. 3. It can be found that the fast fading causes nonideality of the power control, leading to a wider distribution of the SINR.

Both the analytical and simulation results are shown and discussed in the following.

A. Average Data Rate

Fig. 4 plots the analytical and simulation results of the average data rate with 2 or 4 CCs under the JC scheme. The simulations obtain the same results as the analytical solutions in (19). The data rate decreases linearly as traffic load ρ increases. \bar{R} of the JC system with 4 CCs is 2 times of that with 2 CCs because that more CCs are aggregated with the JC scheme, resulting in higher transmission capacity μ .

Numerical results of the average data rate in the IC scheme with various dispatching algorithms are compared in Fig. 5. The obtained \bar{R} of IC-RA is only related to the traffic load ρ as analyzed in (22). Since RA does not help with balancing the traffic on each CC, it can hardly increase the transmission capacity. Therefore, \bar{R} of IC-RA can be regarded as a lower bound. The RR and JSQ algorithms obtain higher throughput, especially when there are more CCs available in the network. The analytical upper bound of RR according to (25) is close to the practical results. As analyzed in Section V, JSQ acquires the best \bar{R} among the three dispatching algorithms.

Fig. 6 plots the average data rates of the DCA scheme, using the SLQ and RRP methods. Both SLQ and RRP obtain the same \bar{R} as the JC scheme, confirming the full utilization of the carrier resources as explained in Section V. Similar to JC, the UEs in the system with 4 CCs also enjoys higher μ data rates than its 2-CC counterpart with the DCA scheme.

B. Normalized Energy Efficiency

The EE performance of the carrier scheduling schemes are shown in Fig. 7. For all the schemes, the NEE decreases when

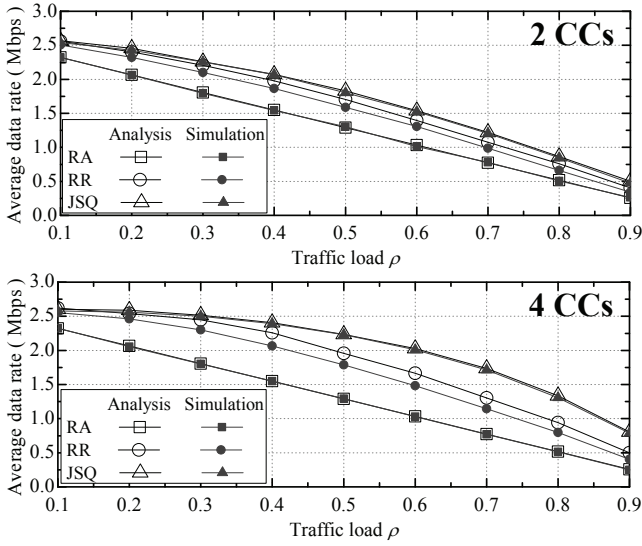


Fig. 5. Analytical and simulation results of the average data rates using the IC scheme with various dispatching algorithms.

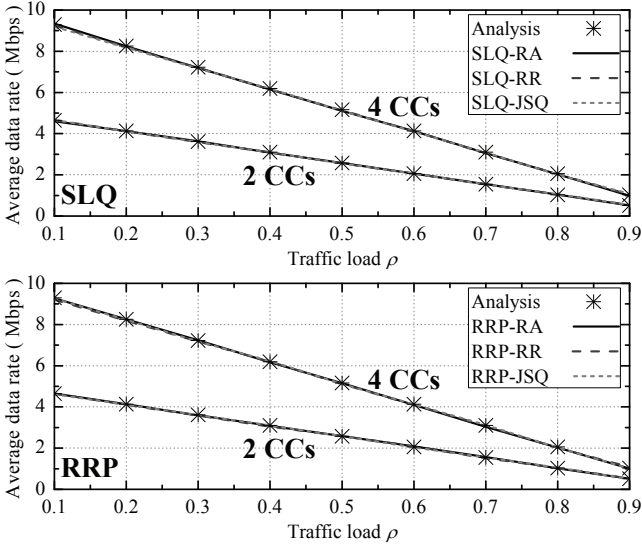


Fig. 6. Analytical and simulation results of the average data rates using the DCA scheme with various dispatching algorithms.

the traffic load becomes higher. The IC-RA scheme has the lowest \bar{R} , while JC incurs the highest power consumption. Thus, they obtain the same worst NEE irrespective of L , which can be regarded as the lower NEE bound. The NEE results of IC-RR and IC-JSQ are better than that of IC-RA, attributed to their balancing effect on the traffic of the CCs that consequently enhances the data rate. The DCA-IBS obtains the best NEE due to its full utilization of radio resources and the ideally balancing mechanism, which can be used as a theoretical upper NEE bound. The SLQ and RRP schemes obtain the same NEE while using the identical dispatching algorithm, outperforming IC and JC. The JSQ method achieves the best balancing effect. It consequently improves the data rate for IC and decreases the energy consumption for SLQ and RRP. When more CCs are available in the uplink system, the NEE of the DCA scheme increases as our analysis.

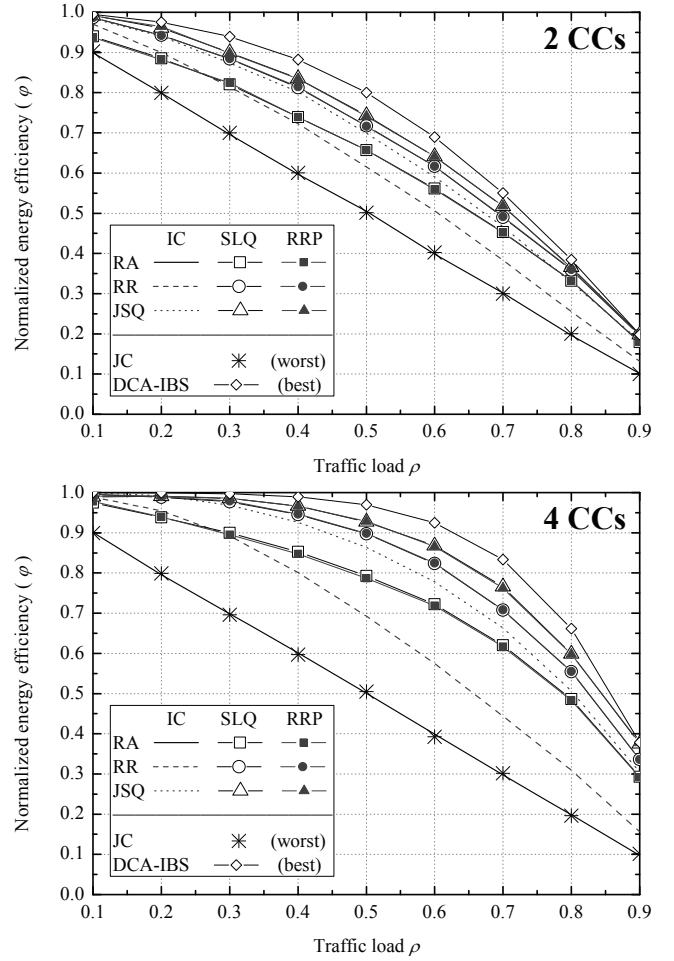


Fig. 7. Analytical NEE values of the DCA-IBS and simulation results of NEE with various schemes and dispatching algorithms.

C. Backward Compatibility and Signalling Overhead

Fig. 8 presents the probability of each UE using only the PCC. With a heavy traffic load, every CC is busy at serving its own flows, and thus nearly no idle CC can be used as the SCC. Therefore, $P\{L^* = 0\}$ is higher with increase of ρ . The IBS acquires the highest $P\{L^* = 0\}$, since the ideally balancing mechanism can reduce the chance of carrier aggregation. As analyzed in (43), (45) and (47), SLQ achieves higher $P\{L^* = 0\}$ than RRP, resulting in better backward compatibility. Specially, in the 2-CC system, their behaviors are the same. The JSQ algorithm helps UEs to obtain more chances to use only the PCC for communications.

Fig. 9 presents the simulation results of the signalling overhead required by the SCC switch procedure when $\rho = 0.5$. The SCC switch frequency in the 4-CC system is higher than in the 2-CC one, since more CCs may be selected as SCCs during their idle periods. SLQ and RRP are the identical DAC scheme for the 2-CC system as mentioned in Section V, so their results are same. The overhead for the SCC switch with SLQ is much higher than RRP in the 4-CC system. The reason is that all the available SCCs are aggregated and switched together by the SLQ scheme, leading to much more overhead.

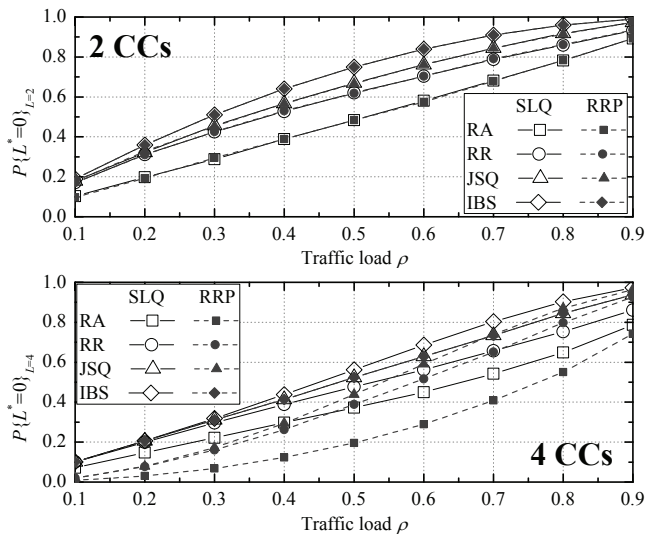


Fig. 8. Analytical values in the IBS and simulation results of the probability of each UE using a single CC with the SLQ and RRP schemes.

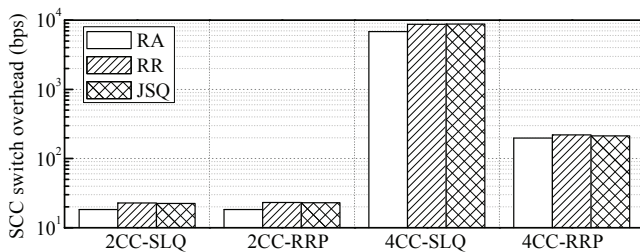


Fig. 9. Comparison of simulation results of the SCC switch overhead of each UE with the SLQ and RRP schemes.

VII. CONCLUSION

In this paper, a dynamic carrier aggregation scheme is proposed to improve the energy efficiency in uplink networks. The JC and IC schemes are introduced as the baseline approaches with poor EE performance. A new EE metric based on bits-per-joule is derived for elastic traffic. The NEE is then proposed for the purpose of universality. Each scheme is analyzed using queuing theory in terms of the data rate and EE. An IBS is built to analyze the upper bound of the performance for the proposed DCA scheme.

Simulation and numerical results suggest that the proposed DCA scheme can efficiently reduce power consumption, while fully utilizing carrier resources to achieve high data rate. Moreover, SLQ has better backward compatibility, and RRP decreases the requirement of the maximum transmit power at UEs and signaling overhead for the SCC switch. In addition, three dispatching algorithms are compared. With more balance capacity of JSQ, the EE of the DCA scheme can be enhanced and even close to that of the IBS. The further analysis and evaluation of the DCA scheme can be extended to the CA-based systems with non-contiguous and heterogenous CCs, which may lead to various transmission capacities of each CC.

REFERENCES

[1] G. Miao, N. Himayat, G. Y. Li, and A. Swami, "Cross-layer optimization for energy-efficient wireless communications: a survey," *Wireless*

Commun. Mobile Comput., vol. 9, no. 4, pp. 529-542, Apr. 2009.

[2] 3GPP TR 36.913 V10.0.0, "Requirement for further advancements for E-UTRA (LTE-Advanced)," Mar. 2011. Online: <http://www.3gpp.org>

[3] 3GPP TR 36.912 V10.0.0, "Feasibility study for further advancements for E-UTRA (LTE-Advanced)," Apr. 2011. Online: <http://www.3gpp.org>

[4] 3GPP TS 36.300, V8.3.0, "E-UTRAN overall description; Stage 2", Dec. 2007. Online: <http://www.3gpp.org>

[5] 3GPP TR 36.814, V9.0.0, "Further advancements for E-UTRA, physical layer aspects", Mar. 2010. Online: <http://www.3gpp.org>

[6] G. Miao, N. Himayat, G. Y. Li, and S. Talwar, "Low-complexity energy-efficient scheduling for uplink OFDMA," *IEEE Trans. Commun.*, vol.60, no. 1, pp. 112-120, Jan. 2012.

[7] A. Akbari, M. A. Imran, R. Hoshyar, and R. Tafazolli, "Average energy efficiency contours for single carrier AWGN MAC," in *Proc. IEEE Vehicular Technology Conference*, 2011, pp. 1-5.

[8] S. Buzzi, G. Colavolpe, D. Saturnino, and A. Zappone, "Potential games for energy-efficient power control and subcarrier allocation in uplink multicell OFDMA systems," *IEEE J. Sel. Topics Signal Process.*, vol.6, no. 2, pp. 89-103, Apr. 2012.

[9] O. Onireti, F. Héliot, and M. A. Imran, "Closed-form approximation for the trade-off between energy efficiency and spectral efficiency in the uplink of cellular network," in *Proc. European Wireless Conf.*, 2011, pp. 706-711.

[10] O. Onireti, F. Héliot, and M. A. Imran, "On the energy efficiency-spectral efficiency trade-off in the uplink of CoMP system," *IEEE Trans. Wireless Commun.*, vol.11, no. 2, pp. 556-561, Feb. 2012.

[11] L. Lei, and K. Zheng, "Performance evaluation of carrier aggregation for elastic traffic in LTE-Advanced systems," *IEICE Trans. Commun.*, vol. E92-B, no. 11, pp. 3516-3519, Nov. 2009.

[12] Y. Wang, K. I. Pedersen, T. B. Sorensen and P. E. Mogensen, "Carrier load balancing and packet scheduling for multi-carrier systems," *IEEE Trans. Wireless Commun.*, vol. 9, no. 5, pp. 1780-1789, May. 2010.

[13] L. Zhang, K. Zheng, W. Wang, and L. Huang, "Performance analysis on carrier scheduling schemes in the long-term evolution-advanced system with carrier aggregation," *IET Commun.*, vol. 5, no. 5, pp. 612-619, Mar. 2011.

[14] G. Berardinelli, T. B. Sorensen, P. Mogensen, and K. Pajukoski, "Transmission over multiple component carriers in LTE-A uplink," *IEEE Wireless Commun.*, vol. 18, no. 4, pp. 67-73, Aug. 2011.

[15] L. Lei, C. Lin, J. Cai, and X. Shen, "Flow-level performance of opportunistic OFDM-TDMA and OFDMA networks," *IEEE Trans. Wireless Commun.*, vol. 7, no. 12, pp. 5461-5472, Dec. 2008.

[16] 3GPP TS 36.213 V10.5.0, "E-UTRA Physical layer procedures," Mar. 2012. Online: <http://www.3gpp.org>

[17] L. Zhang, F. Liu, L. Huang, et al, "Traffic load balance methods in the LTE-Advanced system with carrier aggregation," in *Proc. IEEE Int. Conf. on Communications, Circuits and Systems*, 2010, pp. 63-67.

[18] V. Rodoplu, and T. H. Meng, "Bits-per-Joule capacity of energy-limited wireless networks," *IEEE Trans. Wireless Commun.*, vol. 6, no. 3, pp. 857-865, Mar. 2007.

[19] V. Ramaswami, "The sojourn time distribution in the M/G/1 queue with processor sharing," *J. Appl. Prob.* vol. 21, no. 2, pp. 360-378, 1984.

[20] L. Kleinrock, *Queueing Systems*, vol. 2, John Wiley & Sons, 1976.

[21] V. Ramaswami, "The sojourn time in the GI/M/1 queue with processor sharing," *J. Appl. Prob.* vol. 21, no. 2, pp. 437-442, Jun. 1984.

[22] V. Gupta, M. H. Balter, K. Sigman, and W. Whitt, "Analysis of joint-shortest queue routing for web server farms," *Performance Evaluation*, vol. 64, no. 9-12, pp. 1062-1081, Oct. 2007.

[23] V. Gupta, M. H. Balter, K. Sigman, and W. Whitt, "Simulation results for JSQ server farms with processor sharing servers," *Performance Evaluation*, vol. 64, no. 9-12, pp. 1062-1081, Oct. 2007.

[24] M. Sakata, S. Noguchi, and J. Oizumi, "An analysis of the M/G/1 queue under round robin scheduling," *Operations Research*, vol. 19, no. 2, pp. 371-185, Mar. 1971.

Fei Liu received his B.Eng. degree from the School of Information and Communication Engineering, Beijing University of Posts and Telecommunications (BUPT), China, in 2010. He is currently a candidate for M.S. in the Key Lab of Universal Wireless Communications, Ministry of Education, BUPT. His research interests include performance analysis of wireless networks, resource allocation and scheduling algorithms.





Kan Zheng received the B.S., M.S. and Ph.D degrees from Beijing University of Posts and Telecommunications (BUPT), China, in 1996, 2000 and 2005, respectively, where he is currently an Associate Professor. He worked as a researcher in companies including Siemens, Orange Labs R&D (Beijing), China. His current research interests lie in the field of wireless communications, with an emphasis on heterogeneous networks and M2M/V2V networks.



Hui Zhao received her M.S degree in 2003 from Tianjin University and Ph.D. degree in 2006 from Beijing University of Posts and Telecommunications (BUPT). Since 2006 she has been with the WSPN lab, and now is an associate professor in BUPT, China. She has published more than 20 papers as well as patent applications, and has taken part in a large number of research projects. Her research interests include interference alignment, massive antenna and green communication technologies.



Wei Xiang received the B.Eng. and M.Eng. degrees, both in electronic engineering, from the University of Electronic Science and Technology of China in 1997 and 2000, respectively, and the Ph.D. degree in telecommunications engineering from the University of South Australia in 2004. He currently holds a faculty post of Associate Professor in the Faculty of Engineering and Surveying, University of Southern Queensland, Toowoomba, Australia. His research interests are in the broad area of communications and information theory, particularly coding and signal processing for multimedia communications systems.